Applied Thermal Engineering 31 (2011) 4074–4082

Contents lists available at SciVerse ScienceDirect

Applied Thermal Engineering

journal homepage: www.elsevier.com/locate/apthermeng

Performance evaluations of a geothermal power plant

C. Coskun [a,*], Z. Oktay [a], I. Dincer [b]

[a] Mechanical Engineering Department, Faculty of Engineering, Balikesir University Balikesir, Turkey
[b] Faculty of Engineering and Applied Science, University of Ontario Institute of Technology (UOIT), 2000 Simcoe St. N., Oshawa, ON L1H 7K4 Canada

ARTICLE INFO

Article history:
Received 11 January 2011
Accepted 10 August 2011
Available online 22 August 2011

Keywords:
Geothermal energy
Exergy
Efficiency
Geothermal power plant
Binary plant
Performance parameters

ABSTRACT

Thermodynamic analysis of an operational 7.5 MWe binary geothermal power plant in Tuzla-Turkey is performed, through energy and exergy, using actual plant data to assess its energetic and exergetic performances. Eight performance-related parameters, namely total exergy destruction ratio, component exergy destruction ratio, dimensionless exergy destruction, energetic renewability ratio, exergetic renewability ratio, energetic reinjection ratio, exergetic reinjection ratio and improvement potential are investigated. Energy and exergy losses/destructions for the plant and its units are determined and illustrated using energy and exergy flow diagrams. The largest energy and exergy losses occur in brine reinjection unit. The variation of the plant energy efficiency is found between 6% and 12%. Exergy efficiency values change between 35 and 49%. The annual average energy and exergy efficiencies are found as 9.47% and 45.2%, respectively.

1. Introduction

Geothermal energy appears to be an attractive energy source due to fluctuating oil prices and increasing environmental pollution concerns, including global warming. Since the price of oil has reached its peak and efforts are necessary to find alternative energy resources, the use of geothermal energy is found to be more competitive in comparison to the conventional fossil fuel systems and the direct use of geothermal energy has increased approximately twofold in the last five years [1,2].

Three major types of power plants are widely operated: dry-steam plants, flash-steam plants and binary-cycle plants where the binary and combined flash/binary plants are relatively recent designs. Geothermal energy is used to generate electricity and it finds direct use in areas such as space heating and cooling, industrial processes, and greenhouse heating. High-temperature geothermal resources above 150 °C are generally used for power generation. Geothermal resources that possess moderate temperatures (between 90 and 150 °C) and lower-temperatures (below 90 °C) are best suited for direct use applications [2,3]. Researchers mainly focus on two research areas regarding this issue, which can be expressed as follows: (a) economic evaluation of geothermal power generation [4] and (b) optimum design criteria and suitable working fluids for power cycles [5–13].

Geothermal energy based electricity production for Turkey achieves 100 MWe with six running plants as the first half of 2010. Geothermal power production capacity has increased four-fold within the past four years [14,15]. Table 1 shows existing power plants in Turkey [14,15]. In literature, there have only been a few studies on energetic and exergetic performance parameters for geothermal systems. Specific exergy index, fuel depletion ratio, relative irreversibility, productivity lack and exergetic factor have been introduced [16–19] and applied to geothermal district heating [16,18,20–24]. Lee [17] has proposed the parameter of specific exergy index for some degree of classification and evaluation of geothermal resources using their exergy. Fuel depletion ratio, relative irreversibility, productivity lack and exergetic factor are defined by Xiang et al. [18] for the thermodynamic analysis of some systems. Coskun et al. [22,25] have introduced some system related renewable energy and exergy parameters, namely energetic renewability ratio, exergetic renewability ratio, energetic reinjection ratio, and exergetic reinjection ratio, total exergy destruction ratio, component exergy destruction ratio and dimensionless exergy destruction parameter for geothermal systems. In this study, thermodynamic analysis and performance investigation of Tuzla binary geothermal power plant located in Canakkale, Turkey, are performed using actual plant data. The originality of this study is the first study on investigation of eight energetic-exergetic performance parameters namely; total exergy destruction ratio, component exergy destruction ratio, dimensionless exergy destruction, energetic renewability ratio, exergetic renewability ratio, energetic reinjection ratio, exergetic reinjection ratio and

* Corresponding author. Tel.: +90 266 612 5104; fax: +90 266 612 1257.
E-mail addresses: can.coskun@gmail.com (C. Coskun), zuhal.oktay@gmail.com, Zoktay@balikesir.edu.tr (Z. Oktay), ibrahim.dincer@uoit.ca (I. Dincer).

1359-4311/$ – see front matter © 2011 Elsevier Ltd. All rights reserved.
doi:10.1016/j.applthermaleng.2011.08.013

improvement potential for a geothermal power plant. Also, an application of considering the various outdoor temperature distributions in the exergy calculations is presented for the first time in this study.

2. System description

The geothermal power plant analyzed in this study is a binary designed plant that generates a capacity of 7.5 MWe gross power. The full power production began after the tests in the month of February 2010. The plant operates in a closed loop with no environmental discharge (100% reinjection). The power plant operates on a liquid dominated resource at 175 °C. It utilizes dry-air condensers to condense the working fluid. The geothermal field includes two production wells (T-9, T-16) and two reinjection wells (T-10, T-15). The plant uses isopentane as the working fluid, circulates in a closed cycle. The schematic demonstration and picture of the plant are given in Figs. 1 and 2.

3. Thermodynamic analysis

3.1. Assumptions

The effects of salts and non-condensable gases in the geothermal brine are neglected for calculations. A thermal and physical property of the geothermal water is considered as water in the analyses. EES (Engineering Equation Solver) software program is utilized for the determination of the thermodynamic properties of the geothermal water and isopentane. This program is commonly utilized for the determination of many material thermodynamic properties.

3.2. Analysis

The mass balance for any control volume at steady state can be expressed by

$$\sum_{i=1}^{n} \dot{m}_{in.} = \sum_{i=1}^{n} \dot{m}_{out.} \tag{1}$$

where $\dot{m}$ indicates the mass flow rate. The subscripts in and out indicate the inlet and outlet.

3.2.1. Energy analysis

The energy rate can be expressed by

$$\dot{E}_i = \dot{m}_i \cdot (h_i - h_0) \tag{2}$$

where h indicates enthalpy. Net plant energy efficiency can be described by using the given equation

$$\eta_{sys.} = \frac{\dot{E}_{net}}{\dot{E}_{in}} \tag{3}$$

where, $\dot{E}_{in}$ and $\dot{E}_{net}$ are input and net output energy rates and can be found through

$$\dot{E}_{\text{net}} = \dot{W}_{\text{Turb.}} - \dot{W}_{\text{parasitic load}} \tag{4}$$

$$\dot{E}_{in} = \dot{E}_1 + \dot{E}_6 \tag{5}$$

Here, $\dot{W}_{\text{Turb.}}$ is the electricity production from isopentane cycle. $\dot{W}_{\text{parasitc load.}}$ represents parasitic load. In all plants, there are electrical loads such as pumps fans and controls which are necessary to operate the facility. Often these loads are referred to as "parasitic loads". Air-cooled condenser unit has a great effect on parasitic load and occurs about 60–75% of parasitic loads for investigated system.

The energy efficiency of the isopentane cycle can be described as

$$\eta_{iso.\ cyc.} = \frac{\dot{W}_{\text{Turb.}}}{(\dot{E}_{11} + \dot{E}_{12}) - \dot{E}_{14}} \tag{6}$$

The energy loss for preheater-I and II can be found by

$$\dot{E}_{loss,\ \text{Pre-I}} = (\dot{E}_{18} + \dot{E}_{21}) - (\dot{E}_{20} + \dot{E}_{17}) \tag{7}$$

$$\dot{E}_{loss,\ \text{Pre-II}} = (\dot{E}_{13} + \dot{E}_{17}) - (\dot{E}_{14} + \dot{E}_{16}) \tag{8}$$

The energy efficiency of the pre-heaters can be written as

$$\eta_{\text{Pre-I}} = \frac{\dot{E}_{17} - \dot{E}_{18}}{\dot{E}_{21} - \dot{E}_{20}} \tag{9}$$

$$\eta_{\text{Pre-II}} = \frac{\dot{E}_{16} - \dot{E}_{17}}{\dot{E}_{13} - \dot{E}_{14}} \tag{10}$$

The energy loss and energy efficiency for the turbine become

$$\dot{E}_{\text{loss, Turb.}} = (\dot{E}_{22} - \dot{E}_{21}) - \dot{W}_{\text{Turb.}} \tag{11}$$

$$\eta_{\text{Turb.}} = \frac{\dot{W}_{\text{Turb.}}}{\dot{E}_{22} - \dot{E}_{21}} \tag{12}$$

The energy loss and energy efficiency for the vaporizer are:

$$\dot{E}_{dl.,\ Vap.} = (\dot{E}_{11} + \dot{E}_{12} + \dot{E}_{16}) - (\dot{E}_{13} + \dot{E}_{22}) \tag{13}$$

$$\eta_{Vap.} = \frac{(\dot{E}_{22} - \dot{E}_{16})}{(\dot{E}_{11} + \dot{E}_{12} - \dot{E}_{13})} \tag{14}$$

The energy loss and energy efficiency for two separators (includes expansion valves) are

$$\dot{E}_{lose,\ Sep.} = (\dot{E}_1 + \dot{E}_6) - (\dot{E}_3 + \dot{E}_5 + \dot{E}_8 + \dot{E}_{10}) \tag{15}$$

$$\eta_{Sep.} = \frac{(\dot{E}_3 + \dot{E}_5 + \dot{E}_8 + \dot{E}_{10})}{(\dot{E}_1 + \dot{E}_6)} \tag{16}$$

The energy loss and the energy efficiency for the pumps become

$$\dot{E}_{lose,\ \text{Pump}} = \dot{W}_{\text{Pump}} - (\dot{E}_{out} - \dot{E}_{in}) \tag{17}$$

$$\eta_{\text{Pump}} = \frac{\dot{E}_{out} - \dot{E}_{in}}{\dot{W}_{\text{Pump}}} \tag{18}$$

The energy losses for condenser and the brine reinjection unit are

$$\dot{E}_{lose,\ \text{Cond.}} = \dot{E}_{20} - \dot{E}_{19} \tag{19}$$

$$\dot{E}_{lose,\ \text{Re in.}} = \dot{E}_{15} \tag{20}$$

3.2.2. Exergy analysis

The specific flow exergy (ψ) is given by

$$\psi = (h - h_0) - T_0(s - s_0) \tag{21}$$

Table 1
Geothermal power generation for Turkey.

Power plant	Commissioned in (year)	Installed capacity (MWe)	Max. temperature (°C)
Dora-I Salavatli	2006	7.35	172
Dora-II Salavatli	2010	11.1	174
Ömerbeyli	2009	47.4	232
Bereket	2007	7.5	145
Tuzla-Çanakkale	2010	7.5	171
Kızıldere-Denizli	1984	17.8	243

where T_0,h_0 and s_0 shows the reference temperature, reference enthalpy and entropy, respectively. The subscript 0 stands for dead state. Multiplying specific exergy by the mass flow rate gives the exergy rate:

$$\dot{E}x_i = \dot{m}_i[(h_i - h_0) - T_0(s_i - s_0)] \tag{22}$$

The net plant exergy efficiency is written as

$$\varepsilon_{sys.} = \frac{\dot{E}x_{net}}{\dot{E}x_{in}} \tag{23}$$

where $\dot{E}x_{in}$ and $\dot{E}x_{net}$ are input and net exergy rates as given below:

$$\dot{E}x_{net} = \dot{W}_{\text{Turb.}} - \dot{W}_{\text{parasitc load.}} \tag{24}$$

$$\dot{E}x_{in} = \dot{E}x_1 + \dot{E}x_6 \tag{25}$$

The exergy efficiency of the isopentane cycle is

$$\varepsilon_{iso.\ cyc.} = \frac{\dot{W}_{\text{Turb.}}}{(\dot{E}x_{11} + \dot{E}x_{12}) - \dot{E}x_{14}} \tag{26}$$

The exergy destructions for preheater-I and II are

$$\dot{E}x_{dl.,\ \text{Pre-I}} = (\dot{E}x_{18} + \dot{E}x_{21}) - (\dot{E}x_{20} + \dot{E}x_{17}) \tag{27}$$

$$\dot{E}x_{dl.,\ \text{Pre-II}} = (\dot{E}x_{13} + \dot{E}x_{17}) - (\dot{E}x_{14} + \dot{E}x_{16}) \tag{28}$$

The exergy efficiencies of both pre-heaters are defined as

$$\varepsilon_{\text{Pre-I}} = \frac{\dot{E}x_{17} - \dot{E}x_{18}}{\dot{E}x_{21} - \dot{E}x_{20}} \tag{29}$$

$$\varepsilon_{\text{Pre-II}} = \frac{\dot{E}x_{16} - \dot{E}x_{17}}{\dot{E}x_{13} - \dot{E}x_{14}} \tag{30}$$

The exergy destruction and exergy efficiency for the turbine is

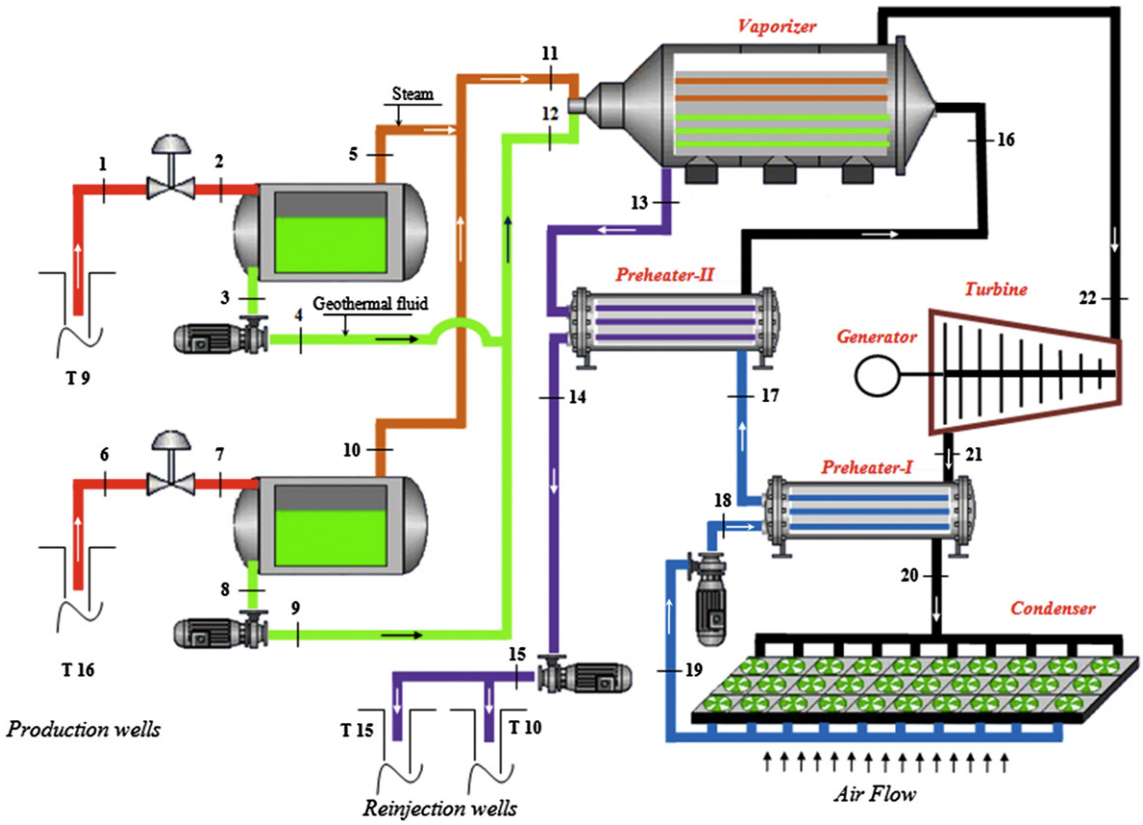

Fig. 1. Schematic layout of the Tuzla geothermal power plant.

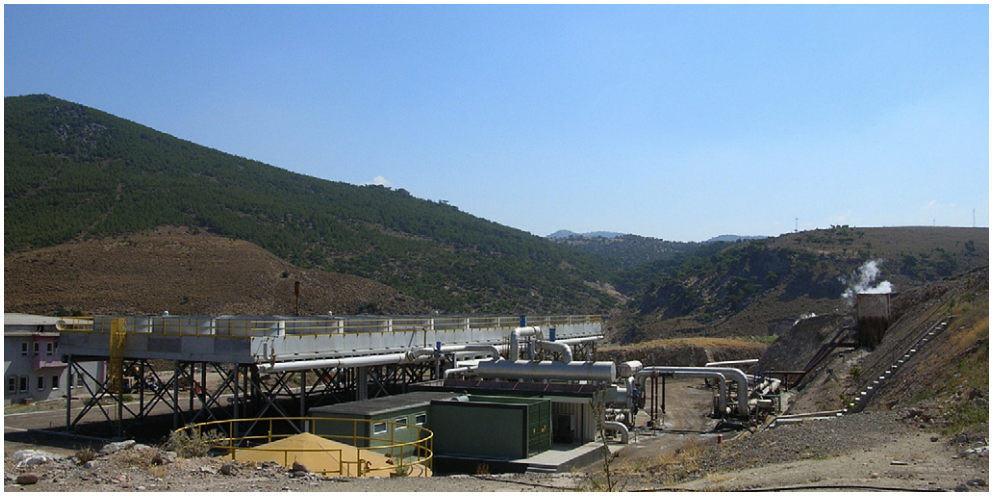

Fig. 2. Tuzla geothermal power plant.

$$\dot{E}x_{dl.,\ \text{Turb.}} = (\dot{E}x_{22} - \dot{E}x_{21}) - \dot{W}_{\text{Turb.}} \tag{31}$$

$$\varepsilon_{\text{Turb.}} = \frac{\dot{W}_{\text{Turb.}}}{\dot{E}x_{22} - \dot{E}x_{21}} \tag{32}$$

The exergy destruction and exergy efficiency for the vaporizer become

$$\dot{E}x_{dl.,\ Vap.} = (\dot{E}x_{11} + \dot{E}x_{12} + \dot{E}x_{16}) - (\dot{E}x_{13} + \dot{E}x_{22}) \tag{33}$$

$$\varepsilon_{Vap.} = \frac{\dot{E}x_{22} - \dot{E}x_{16}}{\dot{E}x_{11} + \dot{E}x_{12} - \dot{E}x_{13}} \tag{34}$$

The exergy destruction and exergy efficiency for the separator (includes expansion valves) are

$$\dot{E}x_{dl.,\ Sep.} = (\dot{E}x_1 + \dot{E}x_6) - (\dot{E}x_3 + \dot{E}x_5 + \dot{E}x_8 + \dot{E}x_{10}) \tag{35}$$

$$\varepsilon_{Sep.} = \frac{(\dot{E}x_3 + \dot{E}x_5 + \dot{E}x_8 + \dot{E}x_{10})}{(\dot{E}x_1 + \dot{E}x_6)} \tag{36}$$

The exergy destruction and the exergy efficiency for the pumps are

$$\dot{E}x_{dl.,\ \text{Pump}} = \dot{W}_{\text{Pump}} - (\dot{E}x_{out} - \dot{E}x_{in}) \tag{37}$$

Table 2
Thermal properties of the plant state and their energy and exergy rates.

State no	Fluid type	Mass flow rate $\dot{m}$ (kg/s)	Temperature T (°C)	Pressure P (kPa)	Enthalpy h (kJ/kg)	Entropy s (kJ/kg°C)	Energy rate $\dot{E}$ (MW)	Exergy rate $\dot{E}x$ (MW)
0	Air	–	25.4	101	25.5	0.089	–	–
0	Isopentane	–	25.4	101	−349.1	−1.687	–	–
0	Water	–	25.4	101	106.6	0.373	–	–
1	GW.	79.11	156.8	570	692.0	1.959	46.311	8.871
2	GW. + S.	79.11	142.8	391	691.8	1.986	46.295	8.218
3	GW.	75.75	142.8	391	601.2	1.769	37.466	5.911
4	GW.	75.75	142.9	772	601.9	1.769	37.519	5.964
5	S.	3.36	142.8	391	2737	6.903	8.838	2.291
6	GW.	23.42	164.2	687	794.0	2.214	16.099	3.233
7	GW. + S.	23.42	142.8	391	793.8	2.231	16.094	3.110
8	GW.	21.31	142.8	391	601.2	1.769	10.540	1.663
9	GW.	21.31	142.9	728	601.8	1.769	10.553	1.676
10	S.	2.11	142.8	391	2737	6.903	5.550	1.439
11	S.	5.47	141.5	377	2735.4	6.915	14.380	3.701
12	GW.	97.06	142.6	550	600.4	1.766	47.928	7.583
13	GW.	102.53	116.5	320	489.1	1.490	39.218	5.043
14	GW.	102.53	90.6	240	379.7	1.200	28.001	2.699
15	GW.	102.53	90.7	540	380.3	1.201	28.062	2.730
16	Isopentane	77.80	103.5	967	−153.2	−1.111	15.241	1.869
17	Isopentane	77.80	49.0	967	−293.3	−1.512	4.341	0.279
18	Isopentane	77.80	32.8	967	−331.6	−1.633	1.362	0.108
19	Isopentane	77.80	32.7	120	−332.4	−1.632	1.299	0.022
20	Isopentane	77.80	38.4	122	16.2	−0.495	28.420	0.747
21	Isopentane	77.80	60.2	126	55.7	−0.376	31.493	1.058
22	Isopentane	77.80	121.4	967	139.9	−0.353	38.044	7.075
A1	Air	3554	25.4	101	25.5	0.089	–	–
A2	Air	3554	33.0	106	33.1	0.115	27.122	0.572

GW: Geothermal water; S: Steam.

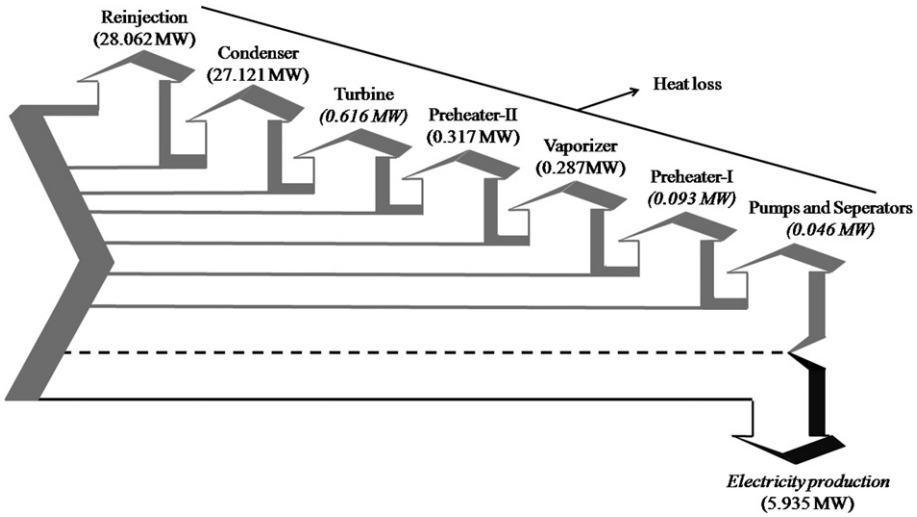

Fig. 3. Energy flow diagram.

$$\varepsilon_{\text{Pump}} = \frac{\dot{E}x_{out} - \dot{E}x_{in}}{\dot{W}_{\text{Pump}}} \tag{38}$$

The exergy destructions for condenser and the brine reinjection unit result in

$$\dot{E}x_{dl.,\ Cond.} = \dot{E}x_{20} - \dot{E}x_{19} \tag{39}$$

$$\dot{E}x_{dl.,\ \text{Re}in.} = \dot{E}x_{15} \tag{40}$$

3.2.3. Energetic and exergetic parameters

Van Gool's improvement potential on rate basis, denoted IP, shows how much potential for improvement exists for the system [16]:

$$IP = (1-\varepsilon)\left[\dot{E}x_{in} - \dot{E}x_{out}\right] \tag{41}$$

Coskun et al. [22,25] have introduced some system related renewable energy and exergy parameters, namely energetic renewability ratio, exergetic renewability ratio, energetic reinjection ratio, exergetic reinjection ratio, total exergy destruction ratio, component exergy destruction ratio and dimensionless exergy destruction parameter for geothermal systems.

The energetic renewability ratio is defined as the ratio of useful renewable energy obtained from the system to the total energy input (renewable and non-renewable altogether) into the system. The energetic renewability ratio for the system is given by below equation:

$$R_{\text{Ren}_E} = \frac{\dot{W}_{Turb.}}{\dot{E}_{in} + \dot{W}_{parasitc\ \ load.}} \tag{42}$$

The exergetic renewability ratio is defined as the ratio of the useful renewable exergy obtained from the system to the total exergy input (renewable and non-renewable altogether) into the system. The exergetic renewability ratio for system is written as follows:

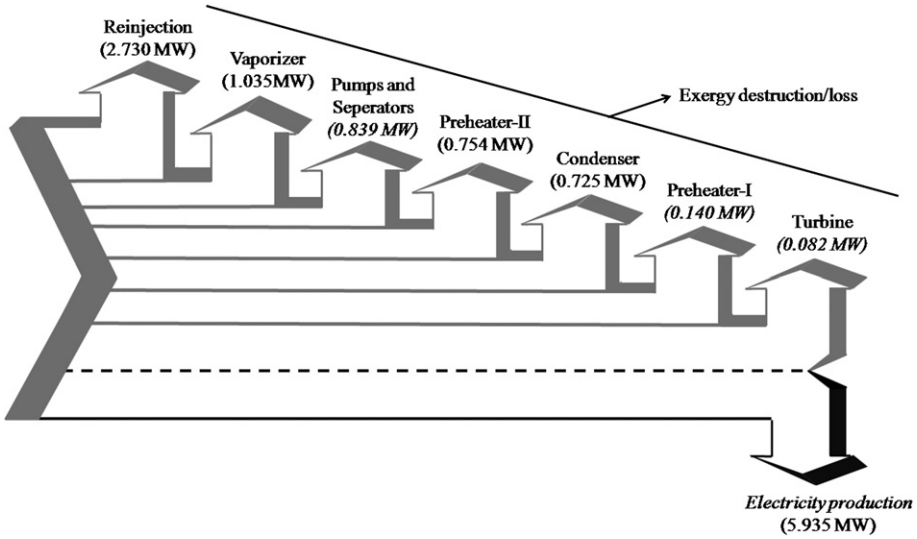

Fig. 4. Exergy flow diagram.

Table 3
Energetic and exergetic performance data of the power plant components.

System component	Heat loses (MW)	Exergy Destruction/Loss (MW)	Energy efficiency (%)	Exergy efficiency (%)	Improvement potential rate (kW)
Vaporizer	0.287	1.035	98.75	83.41	172
Preheater-I	0.093	0.140	96.96	54.97	63
Preheater-II	0.317	0.754	97.17	67.84	242
Turbine	0.616	0.082	90.60	98.60	2
Pumps	0.030	0.038	86.16	82.81	7
Separator I–II	0.016	0.801	99.97	90.24	78
Condenser	27.121	0.725	–	–	–
Reinjection	28.062	2.730	–	–	–

$$R_{\mathrm{Ren}_{Ex}} = \frac{\dot{W}_{Turb.}}{\dot{E}x_{in} + \dot{W}_{parasitc\ \ load}} \tag{43}$$

The energetic reinjection ratio is defined as the ratio of renewable energy discharged to environment or re-injected to the well from the system to the total geothermal energy supplied to the system. The energetic reinjection ratio for system is then

$$R_{\mathrm{Rein}_{E}} = \frac{\dot{E}_{15}}{\dot{E}_{in} + \dot{W}_{parasitc\ \ load.}} \tag{44}$$

The exergetic reinjection ratio is defined as the ratio of renewable exergy discharged to environment or re-injected to the well from the system to the total geothermal exergy supplied to the system. The exergetic reinjection ratio for system is given by below equation:

$$R_{\mathrm{Rein}_{Ex}} = \frac{\dot{E}x_{15}}{\dot{E}x_{in} + \dot{W}_{parasitc\ \ load.}} \tag{45}$$

The total exergy destruction ratio (TExDR) is described as the ratio of total exergy destruction/loss of the system to the total exergy input to the system as given below:

$$TExDR = \frac{\dot{E}x_{Tot.\ \ dl.}}{\dot{E}x_{Tot.\ \ in.}} \tag{46}$$

The component exergy destruction ratio (CExDR) is described as the ratio of exergy destruction/loss of any component of the system to the total exergy input to the system as given below:

$$\mathrm{CExDR} = \frac{\dot{E}x_{i.\ \ dl.}}{\dot{E}x_{Tot.\ \ in.}} \tag{47}$$

where i stands for any component of the system.

The dimensionless exergy destruction (DExD) is described as the ratio of exergy destruction/loss of any component of the system to the total exergy destruction of the system as follows:

$$\mathrm{DExD} = \frac{\dot{E}x_{i.\ \ dl.}}{\dot{E}x_{Tot.,\ \ dl.}} \tag{48}$$

4. Uncertainty analysis

Errors and uncertainties in the experiments can arise from instrument selection, condition, calibration, environment, observation and reading, and test planning [26]. In the present study, temperatures, mass flow rates and pressures were measured and total uncertainties for all these parameters were individually calculated. The accuracy of temperature measuring equipments (temperature transmitters) were ±% 0.675 °C. The accuracy of the mass flow rate (ultrasonic flow matter) was ±%0.5 kg/s. The accuracy of the pressure was ±%1 kPa. According to all these uncertainties and errors, a detailed uncertainty analysis was performed using the method described by Holman [27].

$$U_F = \left[\left(\frac{\partial F}{\partial z_1}u_1\right)^2 + \left(\frac{\partial F}{\partial z_2}u_2\right)^2 + \ldots + \left(\frac{\partial F}{\partial z_n}u_n\right)^2\right]^{0.5} \tag{49}$$

Total uncertainty was carried out for energy and exergy rate as 0.84% and 1.21%, respectively. Also, total uncertainty for energy and exergy efficiency was 1.14% and 1.65%, respectively.

5. Results and discussion

The Tuzla geothermal power plant is investigated for different days and outdoor temperatures. It is found out that two main factors namely; outdoor temperature and operating condition directly affect to energy and exergy efficiency of the system.

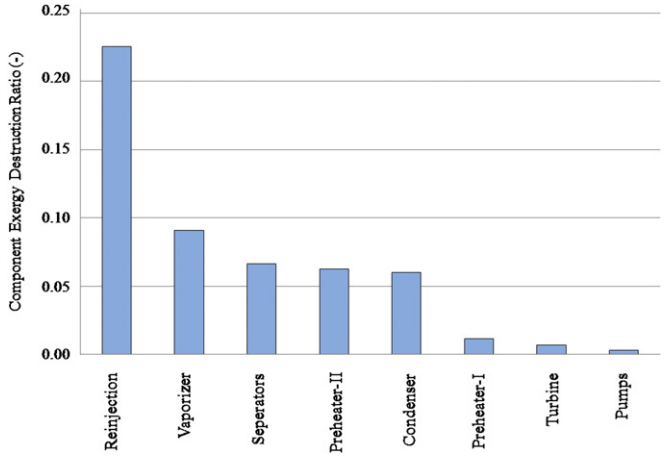

Fig. 5. Component exergy destruction ratio for system components.

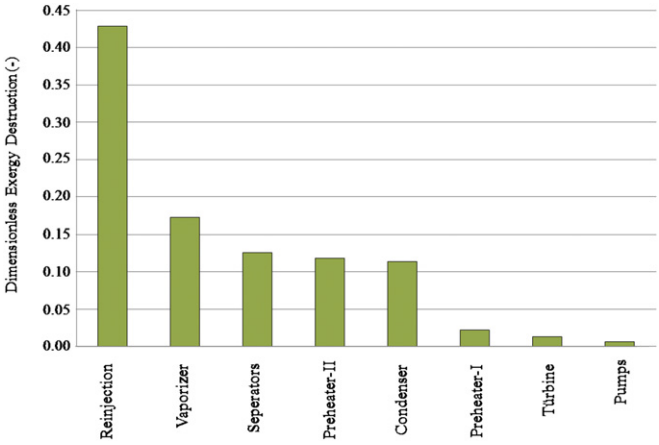

Fig. 6. Dimensionless exergy destruction for system components.

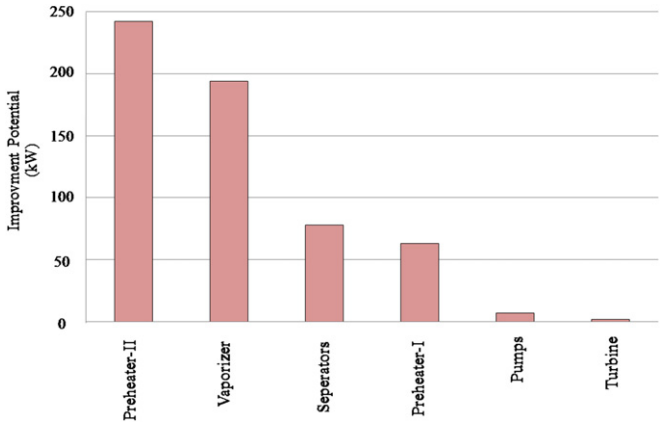

Fig. 7. Improvement potential for system components.

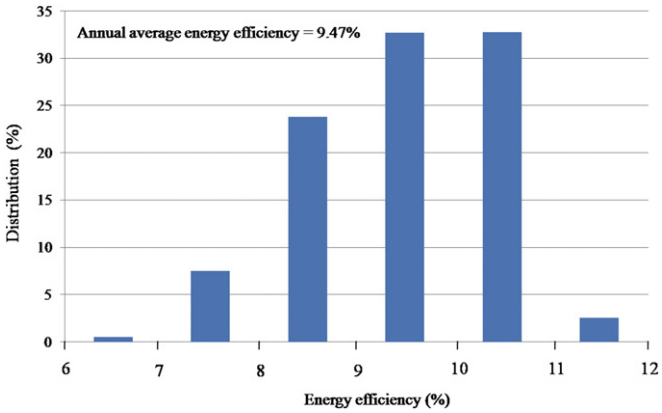

Fig. 8. Distribution of system energy efficiency for annual season.

Outdoor temperature has a dominant effect on system efficiency. New calculation program is written in EES computer program by using actual data. Then, system net energy and exergy functions are determined depend on outdoor temperature as a parameter. These relationships are obtained by the following formulas:

$$\varepsilon_i = 47.52 - 0.0465 \cdot T - 0.00448 \cdot T^2 - 0.000079 \cdot T^3 \quad (50)$$

$$\eta_i = 10.94 - 0.0936 \cdot T - 0.00044 \cdot T^2 - 0.000006 \cdot T^3 \quad (51)$$

where "ε", "η" and "T "stand for the exergy and energy efficiency (%) and the reference environment temperature (°C), respectively. It is found that energy and exergy efficiency values of the system decrease with increasing outdoor temperatures. The design power production capacity of the system is foreseen as 7.5 MW. The daily electricity production capacity is determined by the contract of the daily electricity purchase tender directly placed with the contracted electricity plant and the system is thus provided. Note that the electricity tariff varies depending on on and off-peak hours. As of the period when the investigation was carried out, it was gathered that the electricity selling prices vary between 2 and 25 piaster per kW. The lack of a fixed price agreement constitutes several difficulties during the operation of the system.

The actual operational thermodynamic data for a chosen day are given to show calculation procedure (see in Table 2). Temperature, pressure, mass flow rate, enthalpy, entropy, energy and exergy rates for geothermal water and isopentane are given according to their state numbers as specified in Fig. 1. The exergy rates are calculated for each state with respect to the reference condition of 25.4 °C and 101 kPa (actual temperature and pressure for studied day). Geothermal water enters the vaporizer unit at about 142 °C with a total mass flow rate of 102.53 kg/s. Pre-heaters extract additional heat from the brine by dropping the temperature of the brine down to 90.6 °C. The brine leaving from preheater-II is directed to the reinjection wells and it is re-injected back into the ground. 77.80 kg/s of isopentane circulates through the cycle. Isopentane enters preheater-II at 49 °C and leaves at about 103.5 °C. It then enters the vaporizer and leaves at 121.4 °C. The working fluid then passes through the turbine. The power output from the turbine is 5935 kWe. The working fluid leaving the turbine enters preheater-I at 60.2 °C and leaves at 38.4 °C and then enters to the condenser unit for condensation. Following the condenser unit, the working fluid is pumped to preheater-I at 967 kPa. As of the date that the investigation was carried out, a power production of 5.935 MW has been observed. Parasitic loads for the system is determined as 770 kW. Net power output from the plant obtained by subtracting total parasitic power from the total electricity production. Net energy output is 5.165 MW. The energy and exergy flow diagrams are given in Figs.3 and 4. Some energetic and exergetic performance data for the power plant component are determined and given in Table 3. The improvement potential, energy efficiency, exergy efficiency, heat loss and exergy destruction/loss for each system component are calculated and given in Table 3. The exergy destruction/loss distribution for each component can be determined from the component exergy destruction ratios (CExDR) in Fig. 5. As it can be seen from Fig. 5, exergy destruction for the Brine reinjection unit, Vaporizer, Separators, Preheater-II, Condenser, Preheater-I, Turbine and Pump unit is determined as 22.6, 9.1, 6.6, 6.2, 5.9, 1.2, 0.7 and 0.3% of the exergy input to the plant, respectively. Also, the exergy destruction/loss distribution for each component based on the total exergy destruction/loss can be found by using the dimensionless exergy destruction (DExD) parameter in Fig. 6. Improvement potentials for the system components are calculated and given in Fig. 7. This graphic shows that pre-heaters,

Table 4
Some energetic and exergetic parameters for power plant.

Net plant energy efficiency (%)	8.28
Net plant exergy efficiency(%)	42.67
Energy efficiency of isopentane cycle (%)	17.30
Exergy efficiency of isopentane cycle(%)	69.13
Energetic renewability ratio (−)	0.0865
Exergetic renewability ratio (−)	0.4610
Energetic reinjection ratio (−)	0.4496
Exergetic reinjection ratio (−)	0.2255

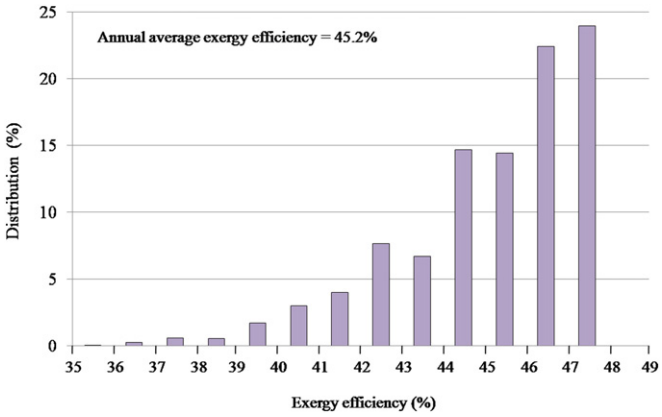

Fig. 9. Distribution of system exergy efficiency for annual season.

vaporizer and separator have high improvement capacity values. These devices can be evaluated and redesigned.

The energy efficiency of the binary geothermal power plants is generally lower than its corresponding exergy efficiency as it varies between 5 and 15%, depending on the temperature of the geothermal source [13,28,29]. Kanoglu [13] has investigated the isopentane utilized as a working fluid power plant. Geothermal source temperature is similar with this study. He investigated net energy and exergy efficiency 8.9% and 34.2%. Following the calculations, the net energy efficiency of the Tuzla geothermal power plant is determined as 8.28%. The energetic and exergetic reinjection ratios are given in Table 4.

The monthly outdoor temperature distribution for Çanakkale is determined using the method proposed by Ref. [30] and then, it loaded to program. The annual energy and exergy distribution appertaining to this reference outdoor temperature distribution is calculated and given in Figs. 8 and 9. There are many studies [31–33] about effect of reference temperature on exergy efficiency in the literature. The application of considering the variant outdoor temperature distributions in the exergy calculations is presented for the first time in this study. It is possible to find monthly average exergy efficiency. Through the utilization of this approach, it is aimed to gain new blood in the determination of the exergy efficiency distribution. The net exergy efficiency of the system varies between 34% and 48%, for annual period taking into account the regional outdoor temperature distribution.

6. Conclusions

The most significant losses in the use of the geothermal fluid have been determined in the reinjection unit as a result of this investigation. It appears that the necessity to reduce the temperature of the utilized geothermal fluid as much as possible becomes evident in order to increase the energetic and exergetic efficiencies of the systems. There is a strong need to enhance the use geothermal options for various applications, such as greenhouse heating, thermal spring path, geothermal heat pump, etc., depending on the temperature levels. Some key findings of the study are listed as follows:

- Considering outdoor temperature distributions, the mean exergy efficiency becomes 45.2% which is 4.77 times greater than the corresponding energy efficiency.
- The highest energy and exergy losses/destructions take place in the brine reinjection unit. If the re-injected geothermal liquid is used, one can provide 16.7 MW for heating and domestic hot water, 3.2 MW for cooling with a single effect absorption cooling system, and 28.3 MW for greenhouse heating. The energetic and exergetic efficiencies of the power plan can be improved by using the integrated multiple generation energy system comprising of heating, cooling and greenhouse heating.
- The present system uses air-cooled condenser units nearby the sea which are affected by drastically by the weather conditions. The efficiencies are then affected. Using water-cooled condensers will eliminate/minimize such potential problems.

To improve geothermal system efficiency, geothermal energy based multi-generation systems and their economic analyses will be conducted in the future.

Acknowledgement

The authors thank Mr. Çığır Diner of plant management for providing plant operation data.

Nomenclature

CExDR	Component Exergy Destruction Ratio (−)
DExD	Dimensionless Exergy Destruction (−)
$\dot{E}$	Energy rate (kW)
$\dot{E}x$	Exergy rate (kW)
h	Specific enthalpy (kJ/kg)
$\dot{I}P$	Improvement potential rate (kW)
$\dot{m}$	Mass flow rate (kg/s)
P	Pressure (kPa)
$\dot{Q}$	Net heat input rate
$R_{\mathrm{Rein}_{Ex}}$	Exergetic reinjection ratio (−)
$R_{\mathrm{Ren}_{E}}$	Energetic renewability ratio (−)
$R_{\mathrm{Ren}_{Ex}}$	Exergetic renewability ratio (−)
$R_{\mathrm{Rein}_{E}}$	Energetic reinjection ratio (−)
s	Specific entropy (kJ/kg°C)
T	Temperature (°C or K)
TExDR	Total exergy destruction ratio (−)
$\dot{W}$	Work input rate (kW)

Greek letters

η	Energy efficiency (%)
ε	Exergy efficiency (%)
ψ	Specific flow exergy (kJ/kg)

Subscripts

Cond.	Condenser
CS	Cooling season
dl	destruction/loss
gw	Geothermal water
HS	Heating season
i	Successive number of elements
in	Inlet
iso. cyc.	isopentane cycle
nd	Discharged to environment or re-injected to the well
out	Outlet
Pre-I	Preheater-I
Pre-II	Preheater-II
Re *in*	brine reinjection unit
Sep.	Separator
Sys.	System
Turb.	Turbine
Tot.	Total
Vap.	Vaporizer
0	Reference (dead) state

References

[1] J. Lund, D. Freeston, T. Boyd. Worldwide direct uses of geothermal energy 2005. In: Proceedings of world geothermal congress, Antalya, Turkey April 24–29, (2005). p. 1–20.
[2] M. Yari, Exergetic analysis of various types of geothermal power plants, Renewable Energy 35 (2010) 112–121.
[3] M. Kanoğlu, A. Bolatturk, Performance and parametric investigation of a binary geothermal power plant by exergy, Renewable Energy 33 (2008) 2366–2374.
[4] M. Kanoğlu, Y.A. Cengel, Economic evaluation of geothermal power generation, heating, and cooling, Energy 24 (6) (1999) 501–509.
[5] A. Borsukiewicz-Gozdur, W. Nowak, Maximising the working fluid flow as a way of increasing power output of geothermal power plant, Applied Thermal Engineering 27 (2007) 2074–2078.
[6] W. Nowak, A.A. Stachel, A. Borsukiewicz-Gozdur, Possibilities of implementation of absorption heat pump in realization of the Clausius–Rankine cycle in geothermal power station, Applied Thermal Engineering 28 (2008) 335–340.
[7] F. Heberle, D. Brüggemann, Exergy based fluid selection for a geothermal organic Rankine cycle for combined heat and power generation, Applied Thermal Engineering 30 (2010) 1326–1332.

[8] A. Schuster, S. Karellas, E. Kakaras, H. Spliethoff, Energetic and economic investigation of organic Rankine cycle applications, Applied Thermal Engineering 29 (2009) 1809–1817.
[9] V.N. Rajaković-Ognjanović, D.Z. Živojinovic, B.N. Grgur, L.V. Rajaković, Improvement of chemical control in the water-steam cycle of thermal power plants, Applied Thermal Engineering 31 (2011) 119–128.
[10] S. Ogriseck, Integration of Kalina cycle in a combined heat and power plant, a case study, Applied Thermal Engineering 29 (2009) 2843–2848.
[11] K.A. Hossain, F. Khan, K. Hawboldt, SusDesign – An approach for a sustainable process system design and its application to a thermal power plant, Applied Thermal Engineering 30 (2010) 1896–1913.
[12] M. Kanoglu, Exergy analysis of a dual-level binary geothermal power plant, Geothermics 31 (2002) 709–724.
[13] M. Yari, S.M.S. Mahmoudi, Utilization of waste heat from GT-MHR for power generation in organic Rankine cycles, Applied Thermal Engineering 30 (2010) 366–375.
[14] U. Serpen, N. Aksoy, T. Öngür. Geothermal Industry's 2009 Present Status in Turkey. In: Proceedings of TMMOB 2nd Geothermal Congress of Turkey (2009) p.55.
[15] U. Serpen, N. Aksoy, T. Öngür, Present status of geothermal energy in turkey, thirty-fifth workshop on geothermal reservoir engineering. Stanford University, Stanford, California, 2010.
[16] W. Van Gool, Energy policy: fairly tales and factualities. in: O.D.D. oares, A. Martins da Cruz, G. Costa Pereira, I.M.R.T. Soares, A.J.P.S. Reis (Eds.), Innovation and technology-strategies and policies. Kluwer, Dordrecht, 1997, pp. 93–105.
[17] K.C. Lee, Classification of geothermal resources by exergy, Geothermics 30 (2001) 431–442.
[18] J.Y. Xiang, M. Cali, M. Santarelli, Calculation for physical and chemical exergy of flows in systems elaborating mixed-phase flows and a case study in an IRSOFC plant, International Journal of Energy Research 28 (2004) 101–115.
[19] L. Ozgener, A. Hepbasli, I. Dincer, Exergy analysis of two geothermal district heating systems for building applications, Energy Conversion and Management 48 (2007) 1185–1192.
[20] Z. Oktay, C. Coskun, I. Dincer, Energetic and exergetic performance investigation of the Bigadic geothermal district heating system in Turkey, Energy and Buildings 40 (2008) 702–709.
[21] A. Hepbasli, A key review on exergetic analysis and assessment of renewable energy resources for a sustainable future, Renewable and Sustainable Energy Reviews 12 (2008) 593–661.
[22] C. Coskun, Z. Oktay, I. Dincer, New energy and exergy parameters for geothermal district heating systems, Applied Thermal Engineering 29 (2009) 2235–2242.
[23] M.A. Rosen, M.N. Le, I. Dincer, Thermodynamic assessment of an integrated system for cogeneration and district heating and cooling, International Journal of Exergy 1 (2004) 94–110.
[24] A. Dagdas, Exergy analysis and pressure optimisation of geothermal binary power plants, International Journal of Exergy 2 (2005) 409–422.
[25] C. Coskun, Z. Oktay, I. Dincer, Investigation of some renewable energy and exergy parameters for two geothermal district heating systems, International Journal of Exergy 8 (1) (2011) 1–15.
[26] E.K. Akpinar, Y. Bicer, A. Midilli, Modelling and experimental study on drying of apple slices in a convective cyclone dryer, Journal Food Process Engineering 26 (2003) 515–541.
[27] J.P. Holman, Analysis of experimental data. in: J.P. Holman (Ed.), Experimental methods for engineers. McGraw Hill, Singapore, 2001, pp. 48–143.
[28] O. Arslan, Exergoeconomic evaluation of electricity generation by the medium temperature geothermal resources, using a Kalina cycle: Simav case study, International Journal of Thermal Sciences 49 (2010) 1866–1873.
[29] A. Franco, M. Villani, Optimal design of binary cycle power plants for water-dominated, medium-temperature geothermal fields, Geothermics 38 (2009) 379–391.
[30] C. Coskun, A novel approach to degree-hour calculation: indoor and outdoor reference temperature based degree-hour calculation, Energy 35 (2010) 2455–2460.
[31] Z. Sogut, Z. Oktay, A. Hepbasli, Investigation of effect of varying dead-state temperatures on energy and exergy analyses of a raw mill process in a cement plant, International Journal of Exergy 6 (2009) 655–670.
[32] Z. Utlu, A. Hepbasli, Parametrical investigation of the effect of dead (reference) state on energy and exergy utilization efficiencies of residential–commercial sectors: a review and an application, Renewable and Sustainable Energy Reviews 11 (2007) 603–634.
[33] C. Coskun, M. Bayraktar, Z. Oktay, I. Dincer, Energy and exergy analyses of an industrial wood chips drying process, International Journal of Low-Carbon Technologies 4 (2009) 224–229.